Abstract

of

The Thesis Entitled

"Design and synthesis of molecules that inhibit cellular enzymes involved in glucose metabolism as anticancer agents"

To be submitted to The Maharaja Sayajirao University of Baroda

For the Degree

of

DOCTOR OF PHILOSOPHY

In Chemistry

By

Gaurav S. Sheth

Under guidance of

Prof. Shailesh R. Shah

Department of Chemistry
Faculty of Science,
The Maharaja Sayajirao University of Baroda,
Vadodara-390002 (India)

Contents

Chapter 1. Introduction

1.1 Pancreatic ductal adenocarcinoma (PDAC)

Pancreatic ductal adenocarcinoma accounts for more than 90% of pancreatic malignancies.[1] It is highly aggressive and lethal malignancy originating from exocrine cells. With a 5-year survival rate of less than 12%, it is one of the leading causes for cancer related deaths worldwide.[2] Majority of PDAC patients are diagnosed at advanced unresectable stages, which contributes to its poor prognosis and low survival rates.[3]

1.2 Current therapies for PDAC

Therapies available for the treatment of PDAC are elaborated in **Table 1**.

Table 1. Current therapies for the treatment of PDAC

Sr. No.	Approved drug	Stage of treatment
1	Gemcitabine	Gemcitabine is a chemotherapy drug that has been a standard treatment for PDAC for many years. It is used in both localized unresectable and metastatic PDAC. It is often combined with other drugs to improve effectiveness.
2	Nab-paclitaxel	Nab-paclitaxel is another chemotherapy drug that is commonly used in combination with gemcitabine for advanced PDAC.
3	FOLFIRINOX	FOLFIRINOX is a combination chemotherapy regimen that includes leucovorin, 5-fluorouracil, irinotecan, and oxaliplatin. It is used for advanced PDAC and has shown improved survival outcomes compared to gemcitabine alone. However, it is generally used in patients with good overall health and functional status due to its increased toxicity.
4	Erlotinib	Erlotinib is a targeted therapy that inhibits the epidermal growth factor receptor (EGFR). It is used in combination with gemcitabine for the treatment of locally advanced, unresectable or metastatic PDAC.
5	Atezolizumab + Bevacizumab	This combination is approved for use in advanced PDAC patients who have not received prior treatment.

Although survival rates of patients with hepatic, gastric and colorectal cancers are increasing due to advancements in treatment, no significant improvement in survival rate is reported for PDAC patients. However, in PDAC, there is a substantial unmet clinical need for novel targeted therapies which should enhance survival and could reduce global mortality rate.[4]

1.3 Reprogrammed tumour metabolism and introduction to malic enzymes

In more than 90% of PDAC cases, mutation in *KRAS* oncogene has been observed. This activates downstream signalling pathways which subsequently regulate cell proliferation, differentiation and apoptosis. PDAC is also associated with deletion of tumour suppressor genes like *INK4A/ARF*, tumour protein 53 (*TP53*), and SMAD family member 4 (*SMAD4*).[5] Tumorigenesis requires adequate supply of energy in the form of ATP and biosynthetic precursors like proteins, nucleic acids and fatty acids.[6] This enhanced requirement in neoplastic cells is satisfied through metabolically rewired processes like aerobic glycolysis, glutaminolysis and elevated fatty acid synthesis. With stimulation of glucose uptake, enzymes involved in glucose metabolism pathway including ones involved in mitochondrial tricarboxylic acid (TCA) cycle are upregulated.

Malic enzymes (MEs) catalyze oxidative decarboxylation of L-malate in to pyruvate and simultaneously reduce $NAD(P)^+$ to NAD(P)H.[7] Three isoforms of malic enzyme have been identified in mammalian context classified based on their cofactor and subcellular localization. ME1 is localized in cytosol and uses $NADP^+$ as cofactor while ME2 is localized in mitochondria and uses $NAD(P)^+$ as cofactor. ME3, a paralogue of ME2, is localized in mitochondria and uses $NADP^+$ as cofactor.[8] Through pyruvate production MEs support generation of lipids and other cellular building blocks. On the other hand, MEs play a crucial role in energy production and redox balance via production of NAD(P)H.

While ME1 expression positively correlates with tumorigenesis in cancers like gastric, breast and squamous cell carcinoma (oral, head and neck) through regulation of NADPH,[9,10,11] ME2 is known to promote survival and proliferation of cancer cells in lung cancer, glioblastoma and oral squamous cell carcinoma.[12,13,14] ME3 overexpression boosts proliferation, migration and invasion capacity of PDAC cells.[15]

1.4 Collateral lethality and role of malic enzyme 3 in PDAC

In 30% of PDAC patients, the tumour suppressor gene *SMAD4* is deleted along with its chromosomal neighbour *ME2*. In this situation ME3 takes over role of ME2. In such patients, inhibition of ME3 will lead to selective death of cancer cells over normal cells where ME2 is operative. Using in vitro and in vivo experiments, Dey *et. al.* have demonstrated that depletion of ME3 in ME2 null PDAC cells (**figure 1**).[16]

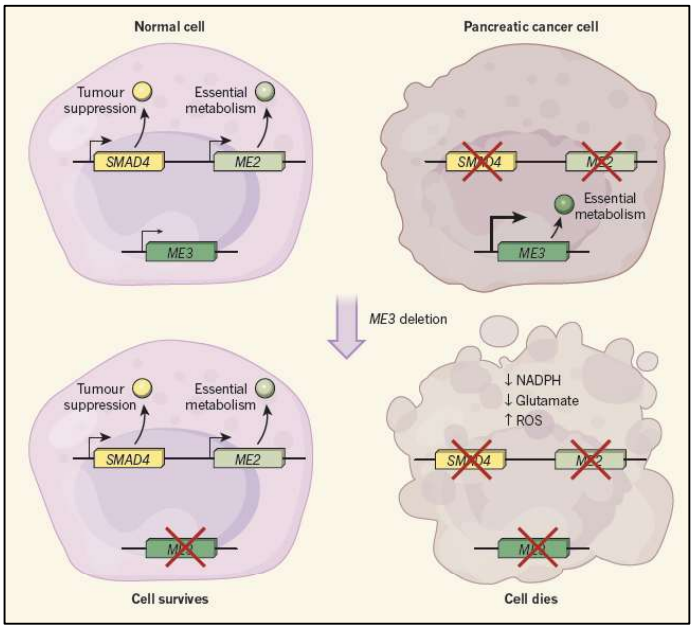

Figure 1. Collateral lethality and role of ME3

ME3 catalyzes conversion of malate in to pyruvate and in this process, it generates NADPH. NADPH is essential in maintaining cellular oxidative stress and redox balance. Inhibition of ME3 will diminish NADPH production and consequently increase reactive oxygen species (ROS) in cancer cells that could possibly lead to apoptosis and cell death. Increased ROS also activates AMP activated protein kinase (AMPK) which supresses sterol regulatory element-binding protein 1 (SREBP1)-directed transcription of branched chain amino acid transaminase 2 (BCAT2). BCAT2 is a transaminase required for branched chain amino acid (BCAA) catabolism hence diminished BCAT2 levels will block nucleotide synthesis which in turn will block proliferation of cells as depicted in **figure 2**.[16]

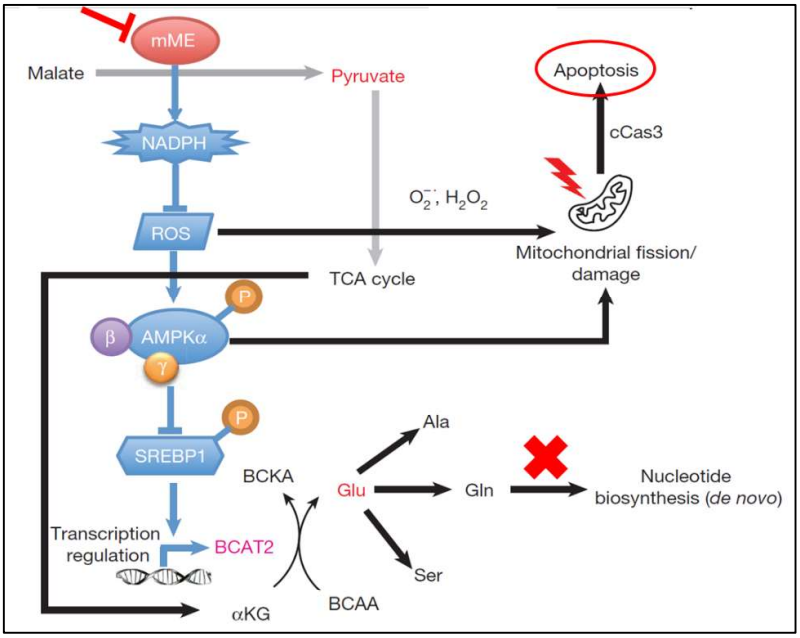

Figure 2. Effect of ME3 inhibition on tumorigenesis in PDAC.

1.5 Objective of research

PDAC is mostly refractory to currently available chemotherapeutic treatments because of limited efficacy. Hence the response rates are often very low. Identification of new molecular targets and subsequent development of effective targeted treatment could increase overall survival rate in PDAC. Based on compelling data published by Dey *et al.*, it was envisaged that selective inhibition of ME3 through small molecule pharmacological inhibitors would create cancer specific metabolic vulnerability leading to cell death. This could be an effective targeted therapy for PDAC patients with deletion of *SMAD4/ME2* genes. Hitherto, no small molecules have been reported as ME3 inhibitors in context of PDAC, hence research was conducted towards identification of first in class hit molecules as ME3 inhibitors which could subsequently be optimized for potency and selectivity.

1.6 Strategy for identification of hits for ME3 as target

Steps taken to find hit molecules for ME3 protein are as follows.

1) ME3 protein crystal structure was not available in protein data base (PDB) so at first human ME3 protein was isolated and purified.
2) Enzyme inhibition assay for ME3 was developed using the purified protein.
3) After that ME3 protein was crystallized as oxalate salt and crystal structure was resolved (1.8 Å).
4) Using this crystal structure, commercial library of 11 million molecules along with SPARC library of 11500 molecules having different chemical scaffolds were docked on malate binding site of ME3 protein.
5) Chemical structures showing good binding affinity and consistent binding mode at malate binding site of ME3 were synthesized using reported methods.
6) Inhibitors of ME1 and ME2 enzymes reported in literature were also synthesized using described methods.[17,18,19,20]
7) Hits from virtual high throughput screening (VHTS) described in step-4 and reported inhibitors of ME1 and ME2 were screened in *in vitro* for ME3 inhibition.

Steps taken are also described as flow chart (**chart-1**).

Chart 1: Flow chart for HIT identification for ME3 protein

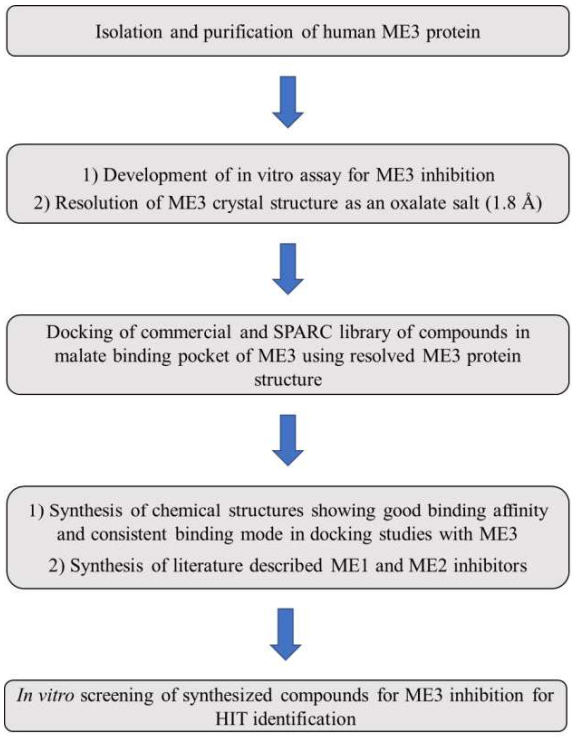

Structures of molecules which exhibited inhibition of ME3 enzyme in *in vitro* screening along with their IC_{50} values are presented in **figure 3**.

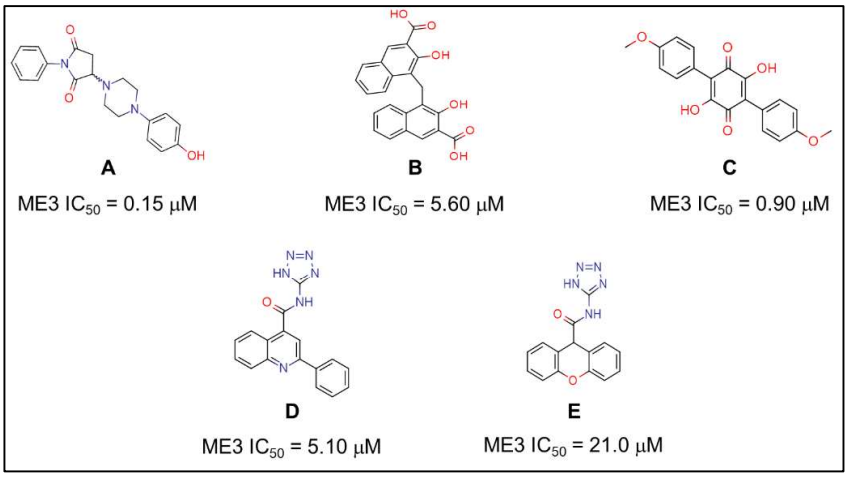

Figure 3: Structures of ME3 inhibitors

1.7 Selection of ME3 hit for further optimization in to lead molecule

Among molecules identified and validated as ME3 inhibitors, compound **A** and compound **C** have exhibited potent inhibition of ME3 enzyme with an IC_{50} value of < 1 µM. From toxicological perspective, quinones are known for producing *in vivo* toxicity. Hence, compound **A** was selected as appropriate scaffold for further optimization in terms of potency and safety over compound **C**.

Chapter 2. Identification of pharmacophore in compound A and study of structure activity relationship.

In silico binding pose of compound **A** (Glide score – 10.03 kcal/mol) in malate binding pocket of ME3 enzyme is presented in **figure 4**. It revealed that **i)** the phenolic hydroxyl group in ring-A forms H-bond donor-acceptor interactions with Asp304 and Asn489 **ii)** ring A was a having cationic···π interaction with the Lys208 side chain and **iii)** the pyrrolidine-2,5-dione ring had an H-bond interaction with Tyr107. Both enantiomers (*R* and *S*) of compound **A** have identical binding modes and interactions with ME3 protein.

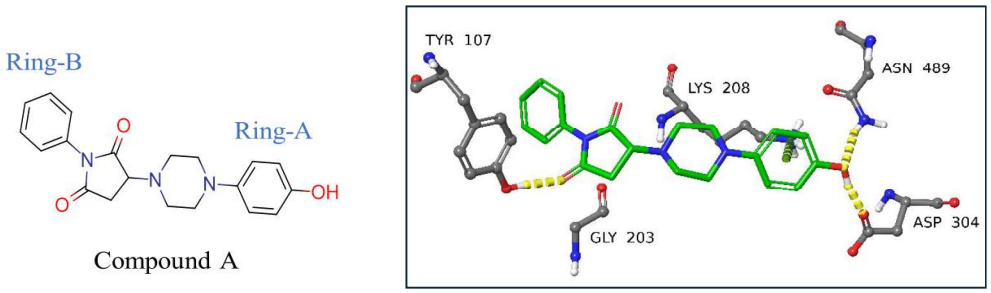

Figure 4. *in silico* binding mode of compound **A** with ME3

2.1 Design strategy – Ring opening and optimization of linker in compound A

Based on binding mode described in **figure 4**, many structures were designed by opening pyrrolidine-2,5-dione ring (compound **1**) and placing different linkers connecting ring-B and the piperidine moiety (compound **2** to **8**) (**figure 5**). Designed compounds (**table 1**) were docked using IFD grid which accommodated compound **A**. All designed compounds retained critical interactions similar to compound **A**. Based on that it was predicted that inhibitory activity on ME3 would be retained. Binding mode of compound **1** with ME3 is depicted in **Figure 6**.

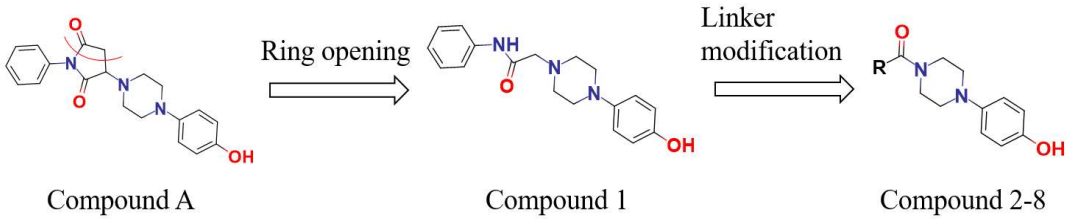

Figure 5. Designing strategy for new molecules

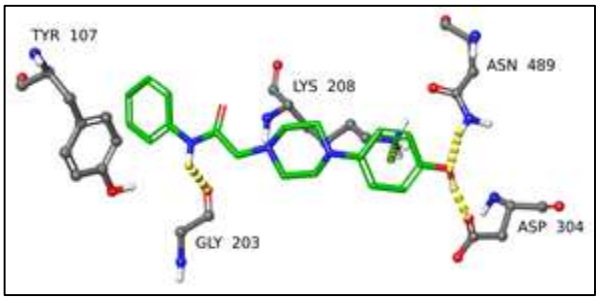

Figure 6. Binding mode of compound **1** with ME3

2.2 Synthesis of newly designed compounds for optimization of linker

Synthesis for these compounds involves following steps.

Scheme 1. Synthesis of piperazine side chains (intermediate III and IV)

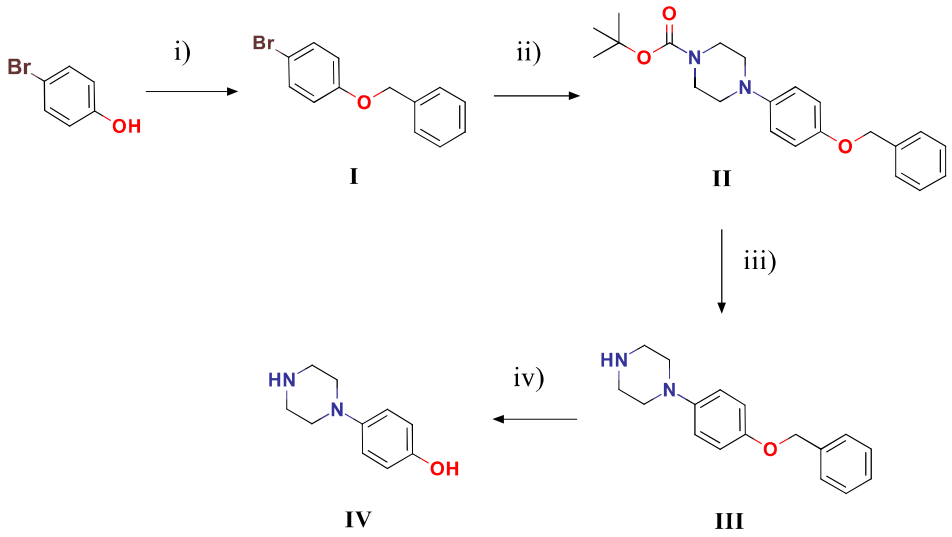

Reagents and conditions: (i) DMF, powdered K_2CO_3, benzyl bromide, 25 °C, 4 h; (ii) *N*-Boc piperazine, sodium *tert*-butoxide, *tetrakis*-(triphenylphosphine)palladium(0), S-Phos, toluene, 90 °C, 3 h, 60-76%; (iii) 1,4-dioxane, conc. HCl, 0-25 °C, 6 h; (iv) 5% Palladium on carbon, H_2, THF-methanol, 25 °C, 6 h.

4-Bromophenol was reacted with benzyl bromide to produce 4-benzyloxy-1-bromobenzene (I). Buchwald-Hartwig coupling between intermediate **I** and N-BOC piperazine yielded tert-butyl 4-[4-(benzyloxy)phenyl]piperazine-1-carboxylate (**II**). **III** was produced by N-BOC deprotection of intermediate II using trifluoroacetic acid. Finally O-benzyl deprotection of **III** by hydrogenolysis using hydrogen / 5% palladium on carbon in tetrahydrofuran:methanol (1:1) produced intermediate **IV**.

Scheme 2. Synthesis of compound 1

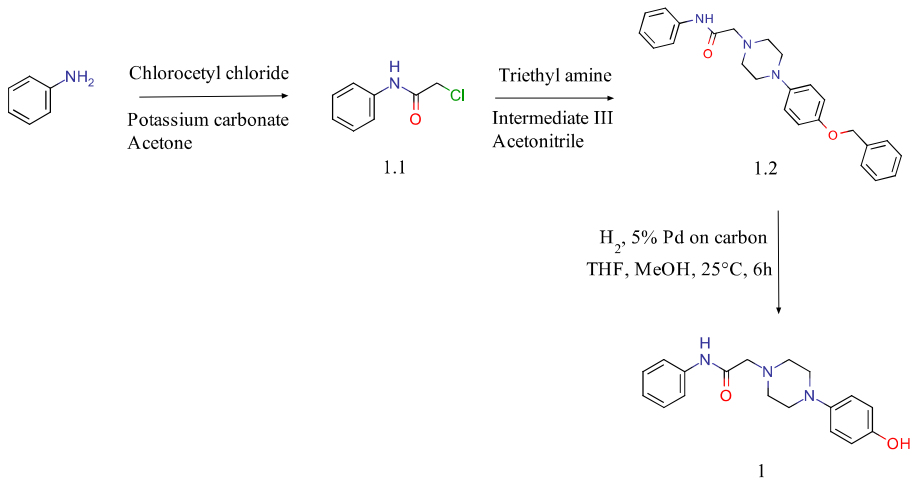

Scheme 3. General synthesis for preparation of urea analogues

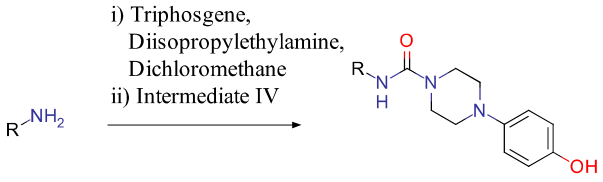

Compound 2; R = phenyl

Scheme 4. General synthesis for the preparation of amide analogues

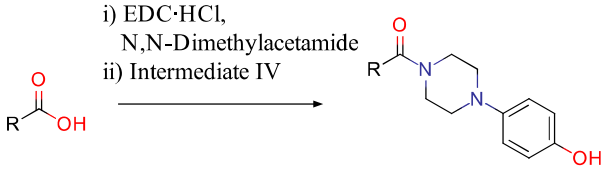

Compound No.	R
3	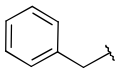
4	
5	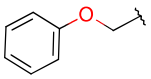

Compound No.	R
6	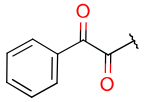
7	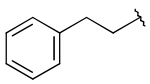
8	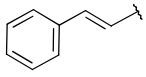

Synthesized compounds were screened in *in vitro* for ME3 inhibitory activity along with other ME isoforms. All compounds **1-8** exhibited promising inhibition of ME3 enzyme similar to that for compound **A (table 1)**. Result indicated that they are pan inhibitors of ME isoforms. Compounds were also screened in *in vitro* for cell growth inhibition of BxPC-3 cells growth inhibition which are *SMAD4/ME2* null pancreatic cancer cell lines. Among them compound **7** has better inhibitory activity of ME3 (IC_{50} = 0.1 μM) along with improved BxPC-3 inhibition (IC_{50} = 3.6 μM).

Table 1. ME isoforms and BxPC-3 cell growth inhibition data for designed compounds

Compound No.	ME3 IC_{50} (μM)	ME2 IC_{50} (μM)	ME1 IC_{50} (μM)	% growth inhibition of BxPC3 cells (10 μM)	BxPC3 cells IC_{50} (μM)
A	**0.15**	**0.20**	**0.22**	**00**	-
1	0.11	0.36	0.34	18	-
2	0.11	0.22	0.20	28	31
3	0.10	0.19	0.18	80	6
4	0.13	-	-	60	-
5	0.13	0.39	0.63	55	-
6	98% at 1 μM	-	-	49	-
7	0.10	0.27	0.27	93	3.6
8	0.08	0.23	0.17	29	-

A second set of urea analogues (**9-14**) was designed wherein lipophilic groups were introduced to improve their cellular permeation and thereby their cellular potency. They were synthesized following general **scheme 3**. Synthesized urea analogues were screened on ME3 enzyme as well as on BxPC-3 cells and results are presented in **table 2**.

Table 2. ME3 inhibition and BxPC-3 cell growth inhibition data for urea analogues

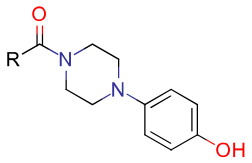

Compound No.	R	% ME3 inhibition		% growth inhibition of BxPC3 cells (10 μM)	BxPC3 cells IC_{50} (μM)
		1 μM	IC_{50} (μM)		
9	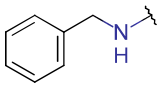	96	0.136	33	-

10	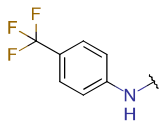	97	0.111	27	-
11	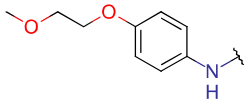	95	0.073	03	-
12	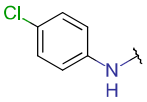	98	0.101	30	`-
13	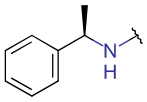	96	-	32	-
14	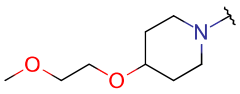	93	-	02	-

Synthesized compounds with urea linker were found to be equipotent in terms of ME3 inhibitory activity but none of the urea analogues were found to be superior to amide analogues *viz.* 3 and **7** in terms of BxPC-3 inhibition.

Similarly, a set of compounds containing amide linker was prepared to increase lipophilicity of molecule for better cell penetration. They were synthesized following general **scheme 4** and screened on ME3 and BxPC-3 (**table 3**).

Table 3. ME3 inhibition and BxPC-3 cell growth inhibition data for amide analogues

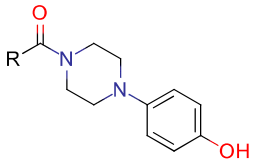

Compound No.	R	% ME3 inhibition		% growth inhibition of BxPC3 cells (10 μM)	BxPC3 cells IC_{50} (μM)
		1 μM	IC_{50} (μM)		
15	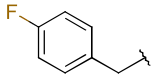	96	0.095	81	6
16	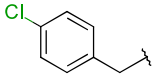	100	0.126	80	5.7

17	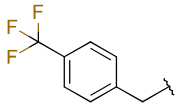	100	-	39	-
18	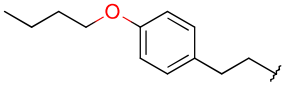	100	0.120	29	`-
19	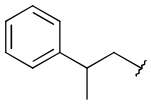	98	-	81	7.4
20	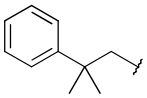	100	0.120	80	5.0

Analysing data generated for urea and amide analogues, it was revealed that amide analogues shows better inhibition of BxPC-3 cell growth compared to urea analogues in spite of having comparable enzymatic activity. Taking together, ME3 enzyme inhibition as well as cellular potency, amide linker was fixed for further optimization of compounds.

2.3 Investigating the role of phenolic hydroxyl group on ME3 inhibition

The binding mode of amide analogue compound **3** in malate binding pocket of ME3 as depicted in **figure 7** revealed that phenolic hydroxyl group provides critical H-bond donor and acceptor interaction with Asp 304 and Asn 489, respectively. To investigate role of phenolic hydroxyl group, next set of molecules **21** to **24** (**figure 8**) were designed and synthesized wherein other polar functionalities were introduced in place of phenol.

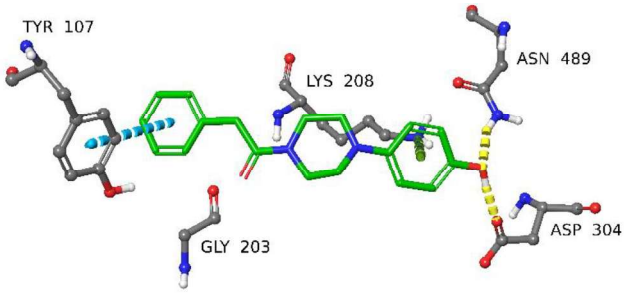

Figure 7. Binding mode of compound **3** with ME3

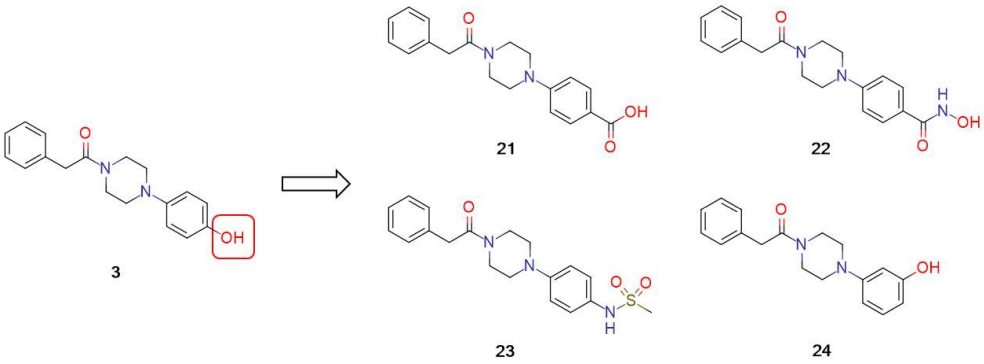

Figure 8. Replacement of phenolic hydroxyl group in compound **3**.

Synthesis of compounds **21**, **22** and **23** was completed as depicted in **schemes 5** and **6**. Compound **24** was synthesized by coupling reaction of commercially available 3-(piperazin-1-yl)phenol with 2-phenylacetic acid using the conditions described in **scheme 4**.

Scheme 5. Synthesis of compounds 21 and 22

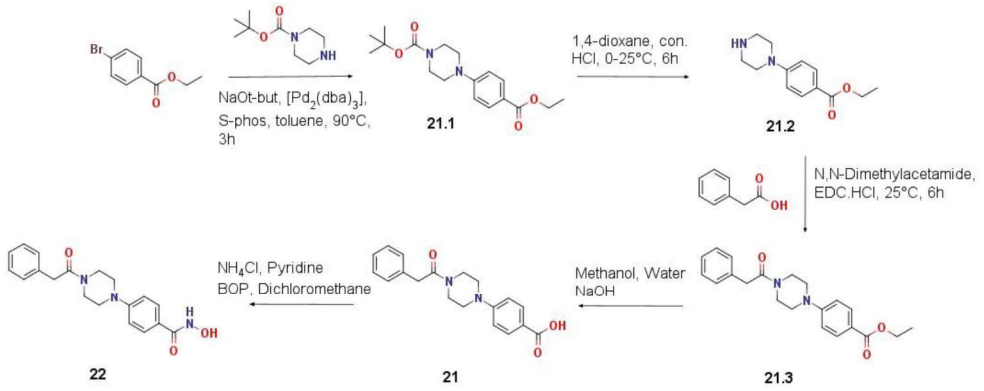

Scheme 6. Synthesis of compounds 23

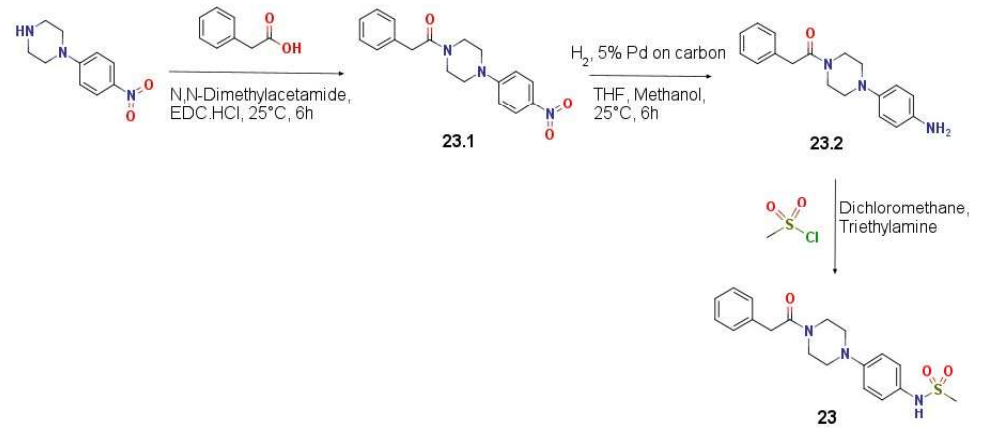

Synthesized compounds **21** to **24** were screened in *in vitro* for ME3 enzyme inhibition and results are presented in **table 4**.

Table 4. Effect of phenolic hydroxyl replacement on ME3 inhibition.

Compound No.	% ME3 inhibition	
	1 μM	10 μM
3	88	100
21	00	19
22	00	15
23	04	32
24	06	00

Results of this study revealed that bioisosteric replacement of phenolic hydroxyl with carboxylic acid, hydroxamic acid or methyl sulphonamide in compound **21**, **22** and **23**, respectively, resulted in loss of activity on ME3. Changing position of phenolic hydroxyl also abolished activity on ME3. Hence it was concluded that phenolic hydroxyl group at position-4 with respect to piperazine is critical for inhibitory potency on ME3.

2.4 Investigating the role of piperazine nitrogens on ME3 inhibition

In the binding mode of compound **3** with ME3, no specific binding interaction was observed for piperazine ring. Hence to investigate importance of piperazine ring, compounds **25** to **27** were designed and synthesized with variants of piperazine ring (**figure 9**).

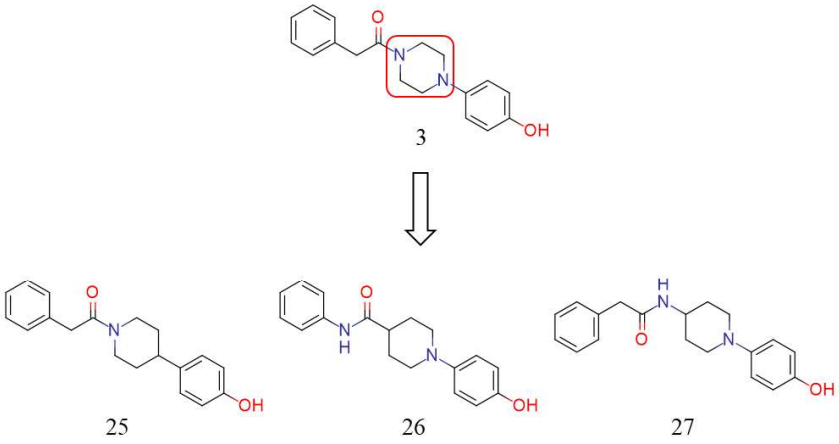

Figure 9. Replacement of piperazine nitrogens in compound **3**.

Compound **25** was synthesized by coupling reaction of commercially available 4-(4-piperidyl)phenol with 2-phenylacetic acid using the conditions described in **scheme 4**. Synthesis of compounds **26** and **27** was completed as depicted in **schemes 7** and **8** respectively.

Scheme 7. Synthesis of compounds 26

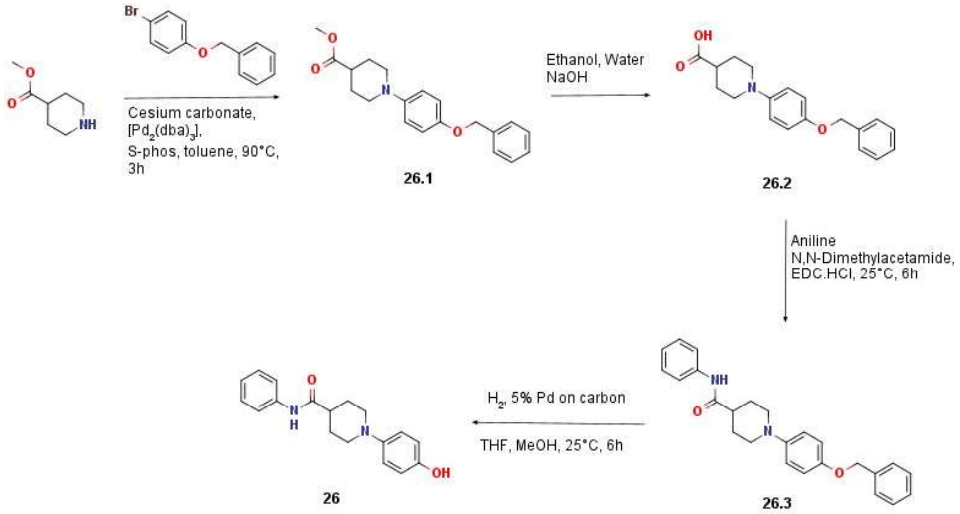

Scheme 8. Synthesis of compounds 27

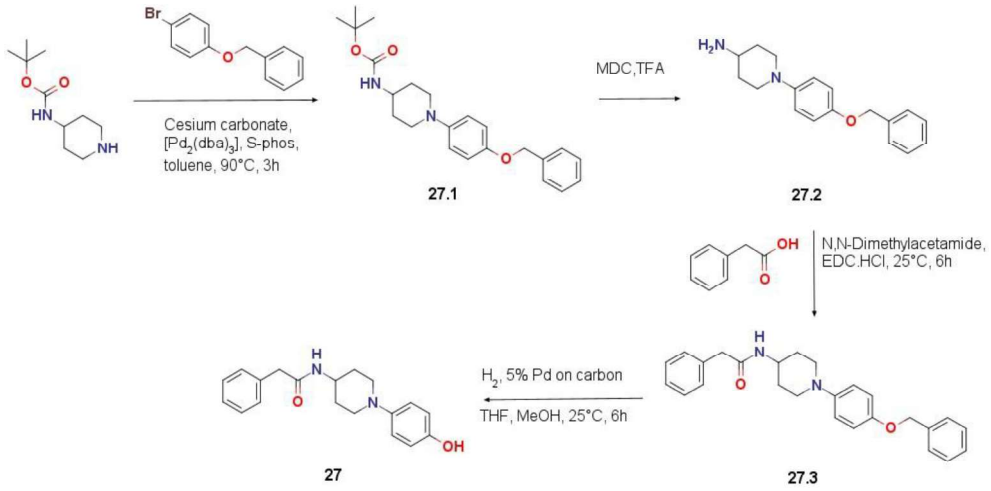

Synthesized compounds **25** to **27** were screened in *in vitro* for ME3 enzyme inhibition as well as on BxPC-3 cell growth inhibition and results are presented in **table 5**.

Table 5. Effect of replacement of piperazine nitrogens on ME3 inhibition.

Compound No.	% ME3 inhibition			% growth inhibition of BxPC-3 cells (10 μM)	BxPC-3 cells IC_{50} (μM)
	1 μM	10 μM	IC_{50} μM		
3	88	100	0.10	80	6
25	13	31	-	-	-
26	100	96	0.13	24	-
27	100	100	0.07	28	-

The results of this study indicated that N-4 nitrogen of piperazine was critical for ME3 inhibition as replacement of N-4 nitrogen with carbon (compound **25**) resulted in significant loss of activity. N-1 nitrogen of piperazine when replaced with carbon in compounds **26** (isonipecotic acid moiety) and **27** (4-aminopiperidine moiety) retained activity on ME3 enzyme. These variants were not superior to compound **3** in terms of BxPC-3 cell growth inhibition.

2.5 Summary

In summary, compound **A** was identified as a hit molecule and was optimized for enzymatic activity and cellular potency which led to potent and cell active ME3 enzyme inhibitors compound **3** and **7** with amide linker. Among these two, compound **7** consisting of the propanamide linker exhibited superior growth inhibition of BxPC-3 cells compared to compound **3** with acetamide linker. The structural elements critical for ME3 inhibition that have been identified are depicted in **figure 10.** These learnings have been utilized for further optimization of molecules.

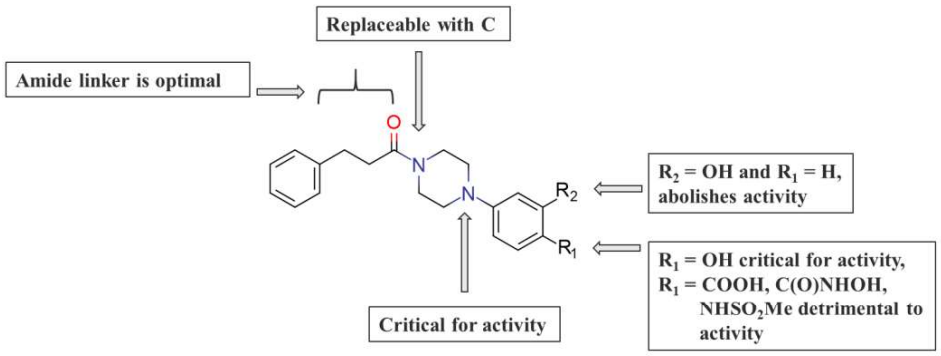

Figure 10. Summary of SAR for ME3 inhibition (Chapter 2)

Chapter 3. Selectivity enhancement for ME3 and in vivo preclinical evaluation.

3.1 Heterocyclic modification to gain selectivity for ME3

Gaining selectivity for ME3 over other ME isoforms was very important for preferential growth inhibition of *SMAD4/ME2* null PDAC cells over normal cells where ME2 is operative. In this regard, replacement of the phenyl ring containing phenolic hydroxyl group (ring-A) with diverse nitrogen containing heterocyclic rings was considered. As per the conceived design, compounds **28** to **32** were synthesized (**Figure 11**).

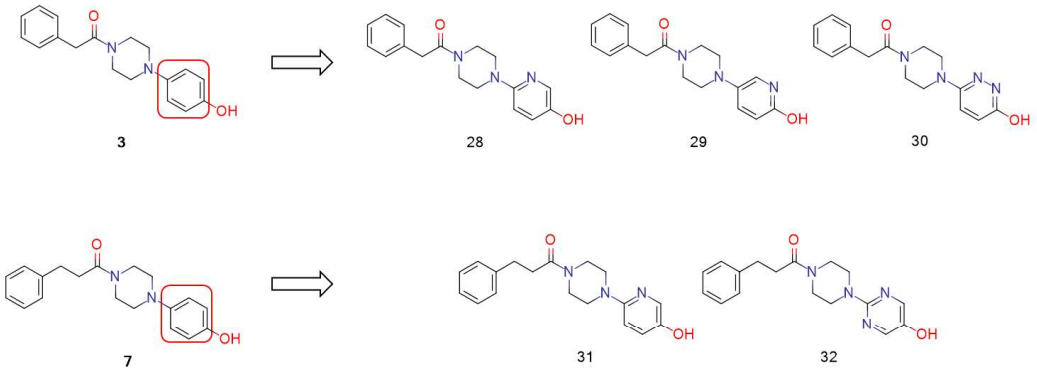

Figure 11. Heterocyclic modification of ring-A in compound **3** and **7**

Compound **28** and **31** were synthesized by coupling of suitable acids with key intermediate **VIII** (scheme **9)**. Pyridine or pyridazine rings with appropriately substituted chloro and hydroxy groups were taken as starting precursors. The same synthetic sequence as for compound **28** was adopted to synthesize compounds **29** and **30** respectively. Similarly, compounds **32** were synthesized using 2-chloropyrimidin-5-ol as starting precursor and following synthesis sequence for compound **31**.

Synthesized compounds **28** to **32** were screened *in vitro* for their inhibitory activity in all ME isoforms and BxPC3 cells (**table 6)**.

Table 6. Effect of heterocyclic modification of ring-A on selectivity for ME3.

Compound No.	ME3 IC_{50} μM	ME2 IC_{50} μM	ME1 IC_{50} μM	BxPC-3 IC_{50} μM
3	**0.10**	**0.19**	**0.18**	**6**
28	0.20	0.98	1.60	7.5
29	Inactive	Inactive	Inactive	-
30	Inactive	Inactive	Inactive	-
7	**0.10**	**0.27**	**0.27**	**3.6**
31	0.23	1.72	1.50	5.10
32	Inactive	Inactive	Inactive	-

The results of this study indicated that replacement of 4-hydroxy phenyl ring (compound **3**) with either 2-hydroxy-5-pyridyl (compound **29**) or 3-hydroxy-6-pyridazinyl ring (compound **30**) resulted in complete loss of activity. However, replacement with 3-hydroxy-6-pyridyl ring (compound **28**) retained activity on ME3 and exhibited 5-fold and 8-fold selectivity over ME2 and ME3 respectively. Similarly, 5-hydroxy-2-pyrimidinyl analogue (compound **32**) of compound **7 was** found to be inactive on ME3 while 3-hydroxy-6-pyridyl analogue (compound **31**) retained potency on ME3 and showed ~7-fold selectivity over ME2 and ME1. Based on inhibitory activity of ME3 enzyme, selectivity over other ME isoforms and BxPC-3 cell growth inhibition, compound **31** was chosen as a new lead for further optimization.

Compound **31** was subjected to docking study with ME3 enzyme and binding mode of compound **31** in malate binding pocket of ME3 (**figure 12**) showed that ring-B was aligned towards hydrophobic pocket of ME3 enzyme.

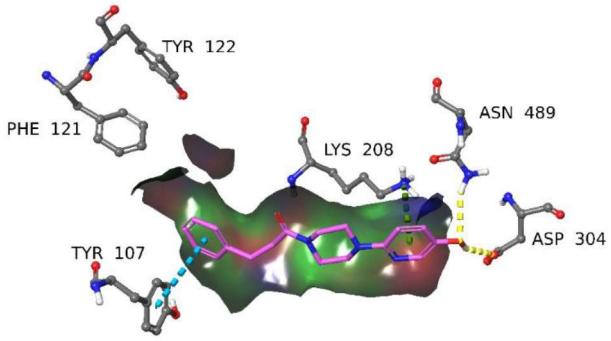

Figure 12. Binding mode of compound **31** in malate binding pocket of ME3

3.2 Lipophilic modification of ring-B in compound 31 to improve ME3 potency

With an intent to improve potency of compound **31,** various analogues with modifications at ring-B were designed and docked in ME3. Compounds with consistent binding modes with ME3 (compounds **33** to **44)** were selected for synthesis (**Scheme 9).**

Scheme 9. Synthesis of pyridine-piperazine side chain (intermediate VIII)

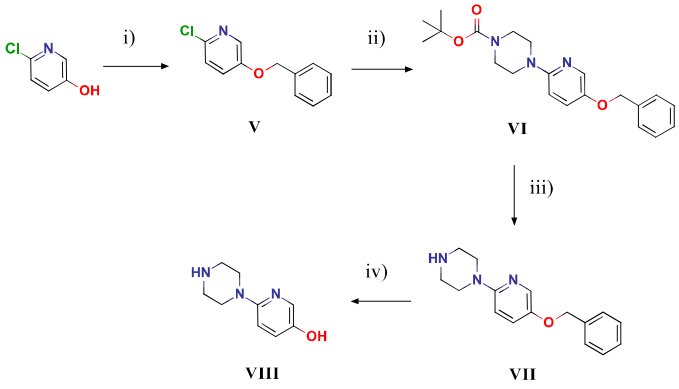

Reagents and conditions: (i) DMF, powdered K_2CO_3, benzyl bromide, 25 °C, 4 h; 80% (ii) *N*-Boc piperazine, sodium *tert*-butoxide, *tetrakis*-(triphenylphosphine)palladium(0), S-Phos, toluene, 90 °C, 3 h, 65%; (iii) 1,4-dioxane, conc. HCl, 0-25 °C, 6 h; 90% (iv) 5% Palladium on carbon, H_2, THF-methanol, 25 °C, 6 h; 85%.

6-chloropyridin-3-ol was reacted with benzyl bromide to obtain 5-(benzyloxy)-2-chloropyridine (**V**). Buchwald-Hartwig coupling between intermediate **V** and *N*-BOC piperazine yielded tert-butyl 4-[5-(benzyloxy)pyridin-2-yl]piperazine-1-carboxylate (**VI**). *N*-BOC deprotection of intermediate **VI** using trifluoroacetic acid produced **VII**. Finally, O-benzyl deprotection of **VII** by hydrogenolysis using 5% palladium on carbon and H_2 in methanol produced the key intermediate **VIII**, which was coupled with suitably substituted acids to produce compounds **33** - **44**. These synthesized compounds were screened in *in vitro* on ME isoforms and BxPC-3 cells (**table 7**).

Table 7. The effect of lipophilic modification of ring-B on ME3 potency

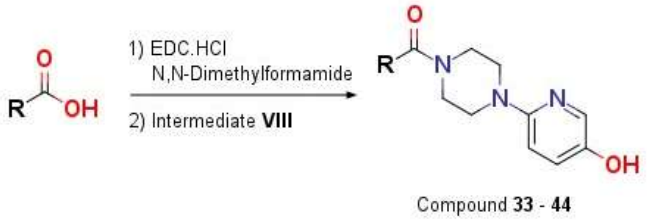

Compound No.	R	ME3 IC_{50} (μM)	ME2 IC_{50} (μM)	ME1 IC_{50} (μM)	% BxPC-3 cell growth inhibition at 10 μM	BxPC-3 IC_{50} (μM)
31	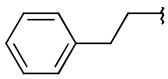	0.23	1.72	1.50	90	5.10
33	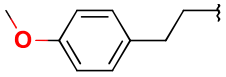	0.47	2.50	1.90	13	-
34	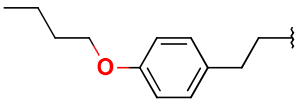	0.39	3.90	1.31	07	15
35	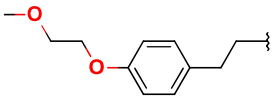	0.58	2.60	3.50	03	-
36	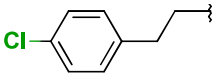	0.14	1.59	1.02	71	6.30
37	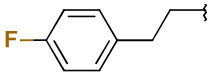	0.41	1.66	1.74	48	-

38	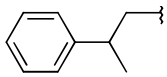	0.17	1.49	0.97	71	4.60
39	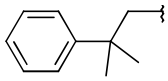	0.15	1.37	2.37	99	3.50
40	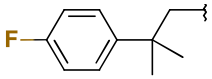	0.31	1.11	1.30	100	5.90
41	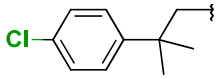	0.36	2.80	1.50	97	5.40
42	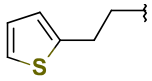	0.16	1.29	1.32	76	4.60
43	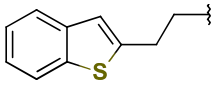	0.24	1.63	1.20	46	-
44	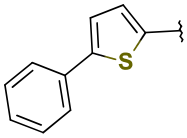	0.25	1.97	1.80	37	-

The results of *in vitro* screening indicated that compounds with methoxy- (**33**), butyloxy- (**34**), 2-methoxyethoxy- (**35**) and fluoro- (**37**) substitution at para position of ring B failed to exhibit any significant advantage, while chloro substitution (**36**) resulted in enhanced potency on ME3 compared to compound **31.** Incorporating –methyl and gem-dimethyl groups at benzylic position of ring-B (*cf.* compounds **38** and **39**) resulted in enhanced potency and selectivity for ME3; however, further substitutions at -*para* position of ring B with fluorine or chlorine (compounds **40** and **41**) resulted in decreased potency. Bioisosteric replacement of phenyl ring B with a thiophene ring (compound **42**) improved the potency on ME3, while replacement with either benzothiophene or 5-phenylthiophene (compounds **43** and **44**) retained the activity on ME3, similar to that of compound **31**.

3.3 Investigating role of logP to improve cellular permeation in BxPC-3 cells.

With an aim to investigate the role of logP on cellular permeability and thereby to improve cytotoxicity on BxPC-3 cells, various analogues with fluoro-, methyl- and trifluoromethyl-substitution on ring-B of compound **31** were designed (compounds **45 - 54**). Key intermediate **VIII** was coupled with suitably substituted acids to produce compounds **45 - 54**. These synthesized compounds were screened in *in vitro* in ME3 enzyme and BxPC-3 cells (**table 8**).

Table 8. ME3 inhibition and BxPC-3 cell growth inhibition data for analogues of compound 31

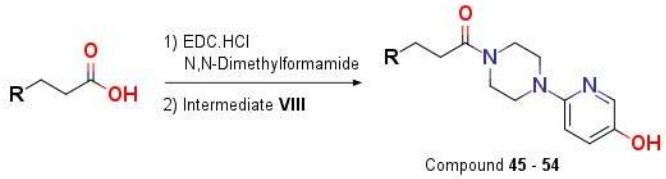

Compound No.	R	% ME3 inhibition		QPlogPo/w*	% growth inhibition of BxPC3 cells (10 μM)	BxPC3 cells IC_{50} (μM)
		1 μM	IC_{50} (μM)			
31	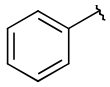	97	0.23	2.51	90	5.10
45	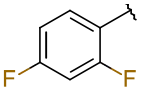	97	0.23	2.79	56	-
46	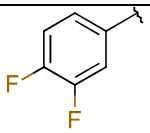	98	0.22	2.79	51	-
47	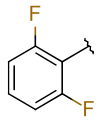	97	0.38	2.79	88	6.9
48	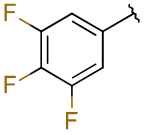	89	0.19	2.94	52	-
49	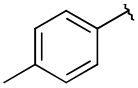	96	-	3.02	54	-
50	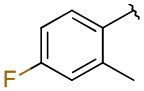	95	0.27	3.16	93	9.8
51	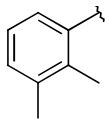	97	0.27	3.53	69	-

52	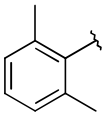	96	0.32	3.53	96	2.1
53	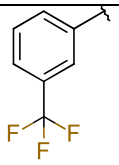	94	-	3.39	29	-
54	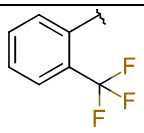	89	-	3.39	31	-

The results of *in vitro* screening revealed that none of the compound except compound **52** (IC_{50} = 2.1 μM) have better potency on BxPC-3 cells than compound **31** (IC_{50} = 5.1 μM) although ME3 inhibitory potency of these compounds is similar.

3.4 Safety evaluation of selected compounds by screening on non-oncogenic cells.

Selected compounds which exhibited good inhibitory potency on BxPC-3 cell growth were screened on non-cancerous cell lines like HCE-T (Human corneal epithelial cell- transformed) and HUVEC (Human Umbilical Vein Endothelial Cells) to evaluate safety margins.

Table 9. Cell growth inhibition data for selected compounds on non-oncogenic cells and BxPC-3

Compound	**Cell lines**		
	Oncogenic (PDAC)	**Non-oncogenic**	
	BxPC-3 IC_{50} (μM)	**HCE-T IC_{50} (μM)**	**HUVEC IC_{50} (μM)**
7	3.6	>30	NA
20	5.0	>30	~30
31	5.1	>30	~30
39	3.5	>30	NA
36	6.3	>30	NA
40	5.9	>30	NA
41	5.4	>30	NA
42	4.6	~25	NA

These compounds were found to have at least 5-6-fold selectivity for BxPC-3 cells over HCE-T cells (**table 9**). Compound **20** and **31** were also found to be selective toward BxPC-3 over HUVEC. These compounds show targeted inhibition of cancerous BxPC-3 cells over non-cancerous cells hence will provide 5-6-fold safety margins in *in vivo* testing.

3.5 In vivo pharmacokinetic (PK) and pharmacodynamic (PD) evaluation of compound 31

At one stage of this development, Compound **31** was selected as a tool compound for *in vivo* xenograft testing based on its biochemical and cellular toxicity data. Hydrochloride salts of compound **31** exhibited very good water solubility. Compound **31-DH** (Dihydrochloride salt of compound **31**) showed water solubility of 50 mg/ml. When refluxed in isopropyl alcohol, compound **31-DH** got converted to its monohydrochloride salt by losing weaker HCl salt with pyridine nitrogen *viz.* compound **31-H** with an improved solubility in water (100 mg/ml). That was another reason of selecting compound **31** which helped to achieve higher dose concentrations in *in vivo* safety and efficacy studies.

3.5.1 In vivo pharmacokinetic (PK) profile

Before testing in *in vivo* xenograft studies, compound **31** and its dihydrochloride salt **31-DH** were investigated for in vivo pharmacokinetic characteristics. These compounds were administered intraperitoneally (ip) at 50 and 100 mg/kg or orally (po) at 200 mg/kg in Athymic Nude mice. The pharmacokinetic parameters of **31** and **31-DH** are presented in **table 10**. Both the molecules possessed acceptable pharmacokinetic properties.

Table 10. PK parameters of compound 31 and compound 31-DH in nude mice (N=3)

Compound	Route of administration	Dose mg/kg	t_{max}(h)	C_{max} (ng/mL)	AUC_{0-t} (ng.h/mL)	$t_{1/2}$ (h)
31	ip	50	0.08	13723	3873	8.5
31	ip	100	0.08	15509	6016	7.1
31	po	200	0.30	7430	3719	1.9
31-DH	po	200	0.25	12256	8338	1.4

3.5.2 In vivo anti-tumour activity evaluation

Compound **31** was evaluated as a tool compound in BxPC-3 subcutaneous xenograft model established in nude mice for its in vivo antitumor potency. It was administered at doses 50, 100 and 200 mg/kg (ip, q.d.) for 37 days which resulted in 48%, 55% and 62% tumor growth inhibition (TGI), respectively. In comparison, current standard of care Gemcitabine, at a dose of 25 mg/kg (ip, q4d) only resulted in 17% TGI. Similarly Nab Paclitaxel, at a dose of 20 mg/kg (ip, q4d) exhibited 41% TGI. Anti tumor effect of compound **31** is visualized by the tumor growth curve in **figure 13**. No body weight loss was observed for tumor bearing mice used for this study, which proved good safety of compound **31**.

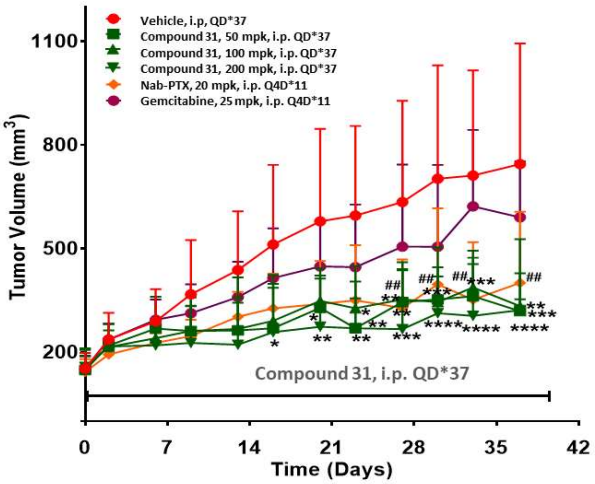

Figure 13. Growth inhibition of BxPC-3 xenografts in mice

3.6 Summary

In summary, the structural elements that are critical for selective ME3 inhibition were identified (**figure 14**) and potent and cell-active ME3 inhibitors that show selectivity over the other ME isoforms were discovered for the first time. Systematic SAR study led to compound **31** which showed improved isoform selectivity, PK profile and good efficacy in animal xenograft model. Overall pre-clinical data suggests that the development of a potent and selective ME3 inhibitor could be a viable therapeutic option for the safe and effective treatment of PDAC.

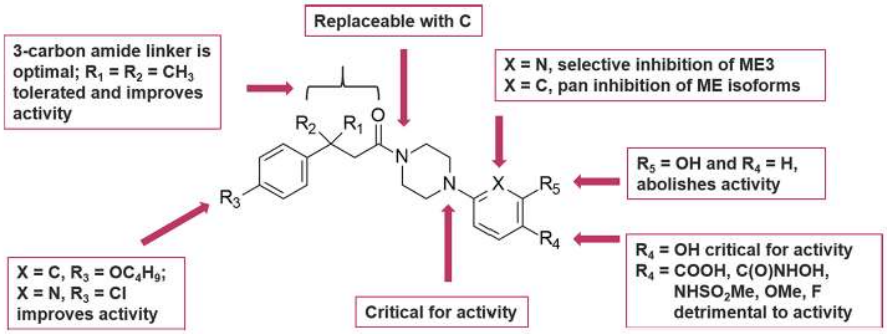

Figure 14. SAR summary for ME3 enzyme inhibition (Chapter 3)

Chapter 4. Design and synthesis of indole-piperazine carboxamide series and in vitro evaluation of tool compound in combination with trametinib

4.1 Structural diversification from compound 31 by incorporating rigidity

With an aim to further improve biochemical potency and cellular inhibition of compound **31**, several new molecules were designed, synthesized and screened for their biological activity. The first step towards optimization of compound **31** was to incorporate structural rigidity in molecule by reducing the number of rotatable bonds. Several structures were designed by **1**) building of bicyclic ring systems through cyclization at α- or β-carbon of the three-carbon linker in compound **31**; and **2**) incorporating small rings between the carbonyl group and ring-B.

1)

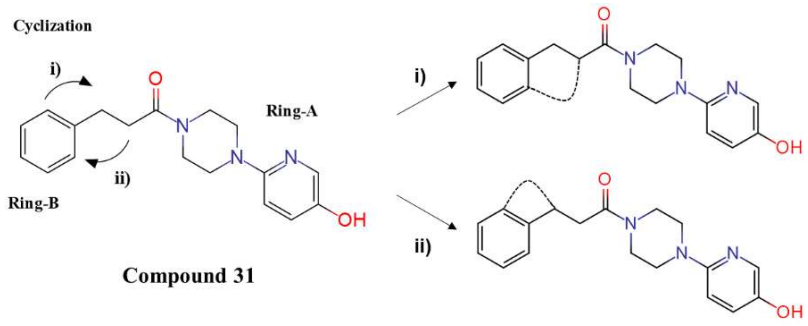

2)

Figure 15. Designing strategy for incorporating structural rigidity in compound **31**

The designed structures were docked in the malate binding pocket of ME3. The *in silico* study predicted that among them, compounds **55** to **59** would retain ME3 inhibitory activity and hence their synthesis was undertaken. Key intermediate **VIII** was coupled with suitably substituted acids to produce compounds **55 - 59**. These synthesized compounds were screened in *in vitro* in ME3 enzyme and BxPC-3 cells (**table 11**).

Table 11. ME3 inhibition and BxPC-3 cell growth inhibition data for compounds have structural rigidity.

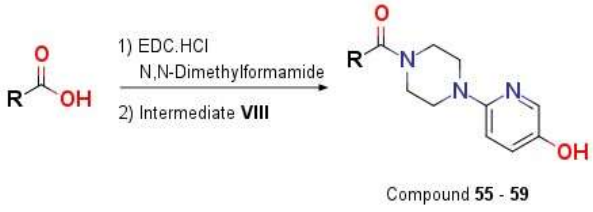

Compound	R	% inhibition of ME3			ME3 IC_{50} (μM)	% inhibition of BxPC-3 cells (10 μM)	BxPC-3 IC_{50} (μM)
		0.1 μM	1 μM	10 μM			
31	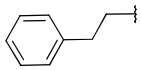	27	97	100	0.23	92	5.2
55	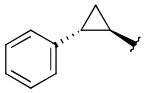	26	91	100	-	18	-
56	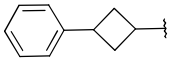	2	93	100	-	21	-
57	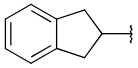	4	94	100	-	22	-
58	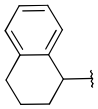	7	92	100	-	22	-
59	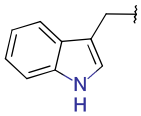	20	93	100	0.25	78	3.7

Obtained *in vitro* screening results were very encouraging as compounds **55** - **59** retained both potency and selectivity for ME3, similar to that for compound **31**. Among them compound **59** with the indolyl moiety was most potent in terms of *ME2*-null BxPC-3 cells (IC_{50} = 3.7 μM) inhibition. After considering the inhibitory potential of compound **59** in biochemical as well as in cell viability assays together, it was selected as the new lead for further development.

4.2 Lead optimization of compound 59 – Indole-piperazine carboxamides

Docking study of compound **59** showed a couple of vital H-bond interactions: **a)** interaction of phenolic hydroxyl group with acid side chain of Asp304; **b)** interaction of indolyl –NH with carbonyl oxygen of val136 main chain (**Figure 16**).

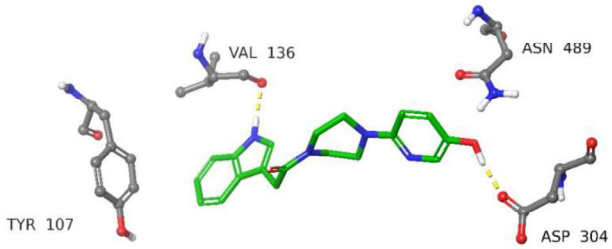

Figure 16. *in silico* binding mode of compounds **59** in the malate binding pocket of the ME3 enzyme.

For further optimization of compound **59**, few analogues with varying linker length and containing halogen substituents were designed and docked in ME3. Structures exhibiting consistent binding modes (compounds **60** - **65**) were taken for synthesis (**table 12**). Analogues **60** and **61** have one methylene carbon less while **64** has one methylene more compared to compound **59**. Compounds **62** and **63** have halogen substituents on indole ring at the position-5 which is metabolically susceptible for hydroxylation. To investigate the role of nitrogen attached hydrogen in the indole ring, Compound **65** was designed as a negative control to study the importance of -NH of indole ring.

Table 12. ME3 inhibition and BxPC-3 cell growth inhibition data for analogues of compound 59.

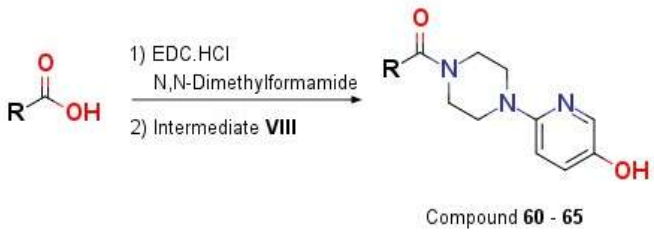

Compound	R	% inhibition of ME3			ME3 IC_{50} (µM)	% inhibition of BxPC-3 cells (10 µM)	BxPC-3 IC_{50} (µM)
		0.1 µM	1 µM	10 µM			
59	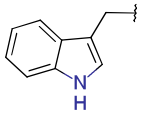	20	93	100	0.25	78	3.7
60	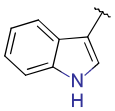	27	97	100	-	45	-
61	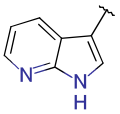	07	90	100	-	16	-

62	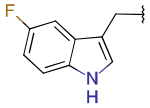	15	96	100	0.21	63	4.8
63	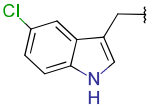	24	97	100	0.21	100	5.4
64	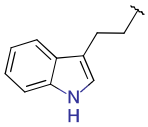	31	96	100	0.25	58	7.7
65	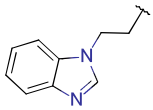	0	67	100	-	0	-

Synthesized compounds **60** - **65** were screened in *in vitro* on ME isoforms for biochemical inhibition and in BxPC-3 cells for growth inhibition (**Table 12**). Compounds **60**, **61** and **64** were found to be equipotent either on ME3 potency or on the growth inhibition of BxPC-3 cells compared to compound **59.** As anticipated, Compound **65** which is devoid of the critical H-bond interaction (N-H···O) with Val136 lost activity both in the biochemical and cellular assays on ME3 enzyme and on BxPC-3 cells respectively. Compound **62** and **63** with 5-halo substitution on indole retained the activity on ME3 as well as on the BxPC-3 cells and this might be advantageous in terms of metabolic stability over compound **59**. Hence, 5-fluoro and 5-chloro indolylacetic acid constructs were fixed in the molecules designed for next round of SAR.

To develop further insight into critical structural features in compound **62**, several designs were made without changing the basic molecular skeleton (**66-71**) as depicted in **Chart 1**.

Chart 1. Structures of compound 62 analogues (variations highlighted in red)

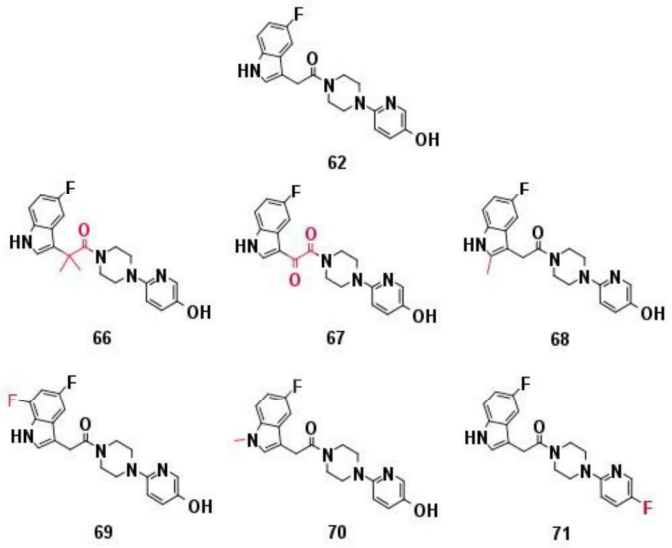

Docking studies were carried out for these modifications with ME3 where it was found that the critical interactions observed for compound **62** with Asp304 and Val136 of ME3 enzyme (**Figure 17**) were retained in compounds **66** to **69.** Methyl substitution on indole-NH (compound **70**) and replacement of the phenolic hydroxyl group with -F (compound **71**) resulted in loss of the essential H-bond interactions with the amino acids as predicted.

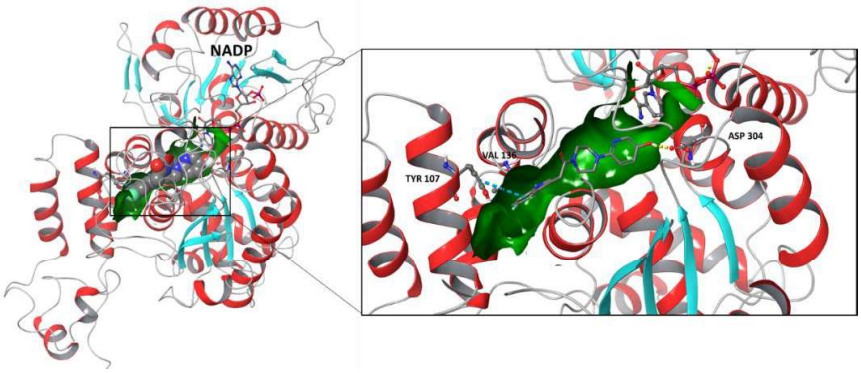

Figure 17. Structure of ME3 protein and *in silico* binding mode of compound **62** in malate binding pocket of ME3

These synthesized analogues were screened on ME3 enzyme and BxPC-3 cells (**Table 13**). As expected compounds **66** to **71** exhibited inhibitory potency on ME3 similar to that exhibited by compound **62.** In concurrence with the *in silic*o predictions, replacement of the hydroxyl group with fluorine (compound **71**) resulted in loss of the inhibitory activity in the ME3 enzyme assay, attributable to the absence of the critical H-bond interaction with Asp 304. however, *N*-methylation of indole ring (compound **70**) retained the inhibitory activity on ME3 enzyme which was not expected. Replacement of amide with an oxoamide (compound **67**) as linker led to enhanced cell growth inhibition of BxPC-3 cells.

Table 13. ME3 inhibition and BxPC-3 cell growth inhibition data for designed compounds

Compound	ME3 IC_{50} (µM)	BxPC-3 IC_{50} (µM)
62	0.210	4.8
66	0.420	4.1
67	0.380	3.0
68	0.420	4.3
69	0.320	4.5
70	0.410	62% at 10 µM
71	32% at 10 µM	ND

To investigate effect of increasing logP on cell growth inhibition, analogues of compound **63** (compound **72** - **74**) were designed and synthesized wherein lipophilic groups were introduced at the positions 2 and 6 of the indole moiety. In biochemical screen for ME3 inhibition, they were found to retain inhibitory potency similar to that of compound **63**. Gradual increase in logP was correlated with the inhibition of cell viability in BxPC3 cells; compound **74** having the highest logP being the most potent (**Table 14**).

Table 14. ME3 and BxPC-3 cell growth inhibition data for compounds 72-74

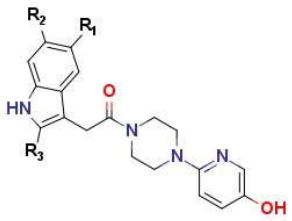

Compound	R_1	R_2	R_3	ME3 IC_{50} (µM)	QPlog Po/w*	BxPC-3 IC_{50} (µM)
63	- Cl	- H	- H	0.210	3.20	5.4
72	- Cl	- H	- Me	0.280	3.53	4.9
73	- Cl	- Cl	- H	0.280	3.59	2.9
74	- Cl	- Cl	- Me	0.320	3.95	2.2

** logP prediction was performed using QikProp*

4.3 In vitro screening of selected compounds in Hs766T PDAC cells

BxPC-3 is a *ME2*$^{-/-}$ PDAC cell line with the wild-type *RAS* genotype while Hs766T PDAC cell line carries *KRAS*, *TP53* and *P16* mutations in addition to *SMAD4/ME2* deletions. In addition Hs766T cells carrying *KRAS*^{Q61H} mutation also exhibit a high level of activated RAS.[21] Due to these reasons Hs766T cells are clinically more relevant with regard to metastatic PDAC. Therefore, the selected compounds exhibiting potent inhibition on BxPC-3 were also screened in Hs766T cells with varying incubation periods viz. short term (96 hours) and long term (2 weeks). In the short- term assay, except for compound **62** (IC_{50} = 11.8 µM), none of the other compounds were found to be active. Similarly, in the long-term assay, compound **62** showed the best potency on Hs766T cells with an IC_{50} of 0.8 µM **(Table 15).**

Table 15. Antiproliferative effect of selected compounds on Hs766T cells

Compound No.		31	59	62	63	66	67	68	72	73	74
Hs766T cells (IC_{50}) µM	2 weeks assay	3.5	2.1	0.8	1.8	2.8	3.0	2.0	2.0	0.9	2.9
	96 hours assay	>30	>50	11.8	>50	>50	>50	>50	>50	>50	>50

4.4 Isobologram analysis for combination of compound 62 and trametinib in Hs766T cells

Combination of drugs is a common practice for clinical management of complex cancers like PDAC. Through comprehensive *in vivo* screening of 57 drug conditions (16 as a single-agent and 41 as two-drug combinations) in genetically engineered KPC mice model, Grbovic-Huezo *et. al.* have demonstrated that a combination of trametinib (MEKi) and PU-H71 (HSP90i) resulted in prolonged survival.[22]

Taking cue from these findings, we sought to investigate the combination effect of trametinib with the most potent of the compounds designed and studied in the current research viz. compound **62** on Hs766T cell growth inhibition in *in vitro*. The combination of compound **62** and trametinib was thought to be synergistic in PDAC because it targets two different pathways that are essential for cancer cell survival. By inhibiting ME3, compound **62** can disrupt cancer cell metabolism and by inhibiting MEK, trametinib blocks the *KRAS* mediated RAS-RAF-MEK pathway. The combination effects of trametinib and compound **62** on Hs766T cells were assessed in *in vitro* using isobologram analysis as it is one of the mathematically proven techniques to evaluate synergistic effect between two drugs (**Figure 18**).

The combination index (CI) was found to be <1 indicating clear synergism between these two compounds.

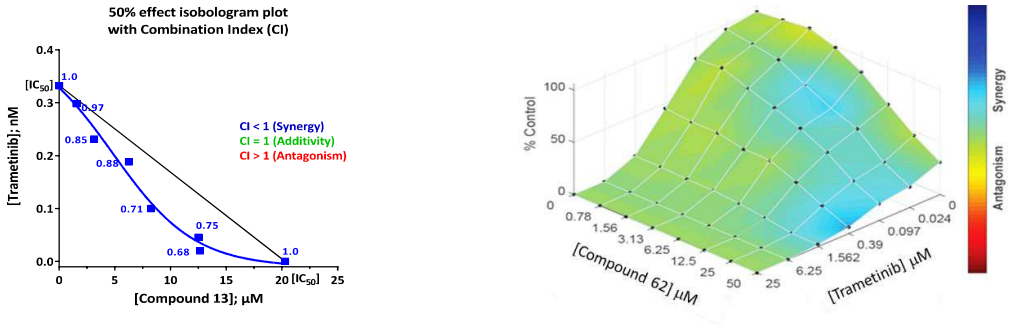

Figure 18. Combination index for compound **62** and trametinib

4.5 Summary

Optimization of compound **31** led to new series of compounds containing indole-piperazine carboxamides. Among them compound **62** exhibited very good inhibitory potency in ME3 (IC_{50} = 0.21 µM) and retained 6-fold and 7-fold selectivity over ME2 and ME1 respectively. Compound **62** showed superior growth inhibitory effects on BxPC-3 as well as on Hs766T PDAC cell lines than compound **31**. When combined with the MEK inhibitor trametinib, compound **62** showed a synergistic effect on Hs766T cell growth inhibition. This combination could be more effective at killing cancer cells than either drug alone.

Chapter 5: Design and synthesis of dual ME3-tubulin inhibitors for the treatment of PDAC

5.1 Designing dual ME3-tubulin inhibitors for enhanced cell growth inhibition of PDAC cell lines.

Microtubules play a crucial role in multiple cellular function like cell division, mitosis, signal transmission, angiogenesis etc.[23] Hence, drugs targeting microtubule are highly successful as chemotherapeutic agents. Albumin bound paclitaxel (nab-PTX) in combination with gemcitabine is current standard of care for PDAC as a first line therapy. It works with an impact on the stabilization of microtubule.

In literature molecules depicted in **Figure 19** are described as small molecule tubulin inhibitors.[24,25] There is a remarkable structural similarity between these molecules and the molecules we have identified as ME3 inhibitors. Both contains similar piperazine carboxamides moiety. Taking cue from their structural features and our identified ME3 inhibitors, diverse series of piperazine carboxamides was designed as dual tubulin - ME3 inhibitors by combining key structural features of both the series together. The idea was that ME3 and microtubule dual inhibition would have superior cytotoxic effect on PDAC cells.

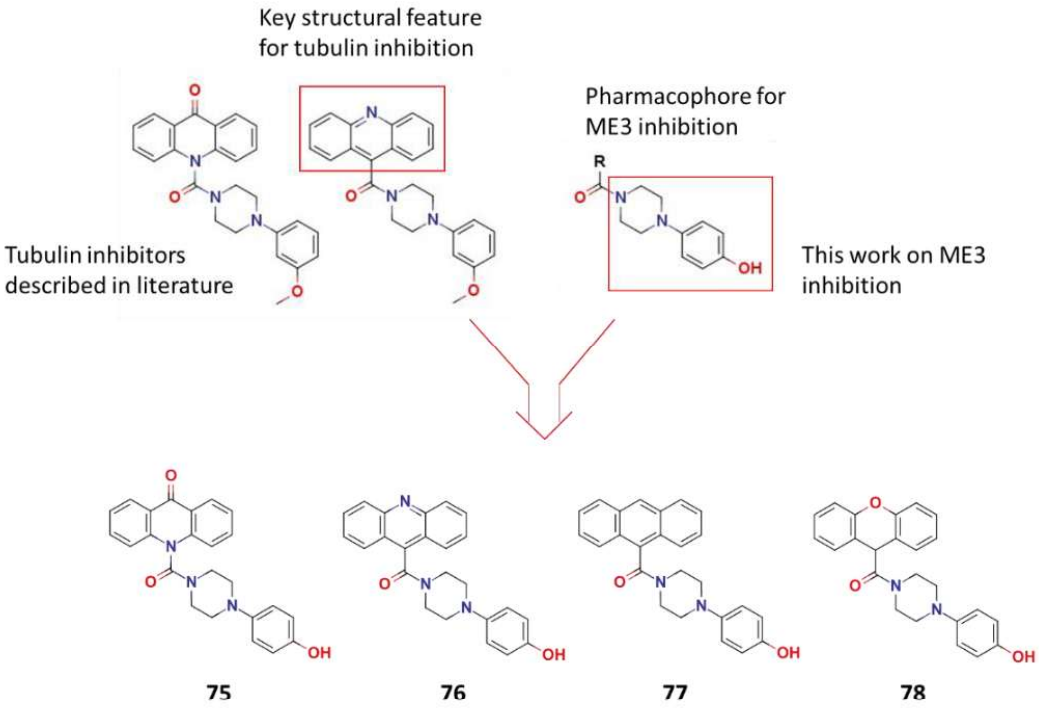

Figure 19. Designing of dual Tubulin - ME3 inhibitors

5.2 Synthesis and biological evaluation of the designed compounds and related SAR.

Compounds **76-78** were synthesized by coupling of suitable acids with intermediate **IV** following general **scheme 4** while compound **75** was synthesized following procedure reported by Waltemate *et. al* for similar analogues.[25] Synthesized compounds were screened in ME3 enzyme inhibition and BxPC-3 cell growth inhibition assays (**Table 16**).

Table 16. ME3 inhibition and BxPC-3 cell growth inhibition data for tricyclic compounds 75-78.

Compound	ME3 IC_{50} (µM)	BxPC-3 IC_{50} (µM)
75	0.150	0.320
76	0.095	0.106
77	0.152	1.1
78	40% at 0.1 µM	56% at 10 µM

As expected compounds **75** and **76** exhibited potent inhibition of ME3 and gained potency in terms BxPC-3 cell growth inhibition having sub nanomolar IC_{50} values. This transition of BxPC-3 IC_{50} values from micromolar to sub nanomolar range was supposed to come from engaging tubulin as a target. This proves that these compounds work by dual mechanism of action engaging ME3 as well as tubulin as targets. Compound **77** and **78** exhibited comparable ME3 inhibitory potency but were inferior in terms of BxPC-3 cell growth inhibition.

Compounds listed in **Table 17** were designed to generate SAR around compounds **75-77**. In compound **79**, linearly fused anthracene ring in compound **77** was replaced with angularly fused phenanthrene ring. Position of the carboxamide bond in compound **77** was changed from 9-position to 1-position of anthracene ring in compound **80** to evaluate its positional importance. To assess the significance of linearly fused tricyclic ring, acridine ring in compound **76** was replaced with a 1,2,3,4-tetrahydroacridine ring and 2-phenylquinoline ring in compound **81** and **82** respectively. Compound **83** was designed by introducing one carbon spacer between acridone ring and carbonyl group in compound **75** to assess the importance of rigidity. Phenolic hydroxyl group of compound **76** was replaced with methoxy group (compound **84**) to estimate how much contribution of BxPC-3 cell growth inhibition comes from ME3 depletion. Designed compounds were synthesized and screened in ME3 enzyme inhibition and BxPC-3 cell growth inhibition assays (**Table 17**).

Table 17. ME3 inhibition and BxPC-3 cell growth inhibition data for designed compounds 79-84

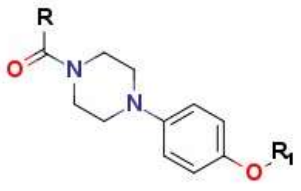

Compound	R	R_1	% inhibition of ME3			ME3 IC_{50} (µM)	BxPC-3 IC_{50} (µM)
			0.1 µM	1 µM	10 µM		
79	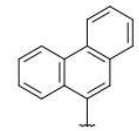	-H	57	100	100	-	53% at 10 µM
80	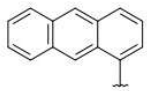	-H	35	99	100		24% at 10 µM
81	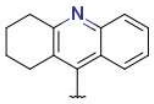	-H	18	98	100	-	57% at 10 µM
82	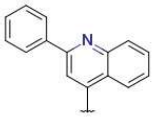	-H	67	100	100	0.138	21% at 10 µM
83	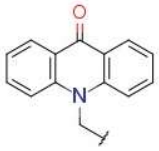	-H	28	100	100	0.220	5% at 10 µM
84		$-CH_3$	0	0	0	-	1.4

The results of *in vitro* data revealed that compounds **79**-**83** retained activity on ME3 but failed to show sub nanomolar inhibition of BxPC-3 cell growth. This could be attributed to probable loss of activity on tubulin front. In vitro data for compound **79** and **80** showed that linearly fused tricyclic ring attached from 9-position is critical in terms of tubulin inhibition and subsequent inhibitory potency on BxPC-3 cells. Analogues of compound **76** wherein: i) saturation of one ring in tricyclic acridine ring was carried out (compound **81);** and ii) acridine ring was replaced with 2-phenylquinoline (compound **82**), resulted in loss of activity on BxPC-3 cells. Flexible analogue of compound **75** with one more carbon spacer between acridone ring and carbonyl group (compound **83**) also resulted in loss of activity on BxPC-3 cells. These findings suggest that these modifications are not favourable in terms of tubulin inhibition and related impact on BxPC-3 cells.

As expected compound **84** lost its activity on ME3 enzyme and steep decrease was observed in inhibitory potential on BxPC-3, from sub nanomolar to micromolar. This proves that sub nanomolar activity on BxPC-3 for compound **76** can be attributed to its capability to engage two different targets (ME3 and tubulin).

Compounds **75** and **76** showing potent inhibition of BxPC-3 cells were also screened in other pancreatic cell lines where they have exhibited potent impact on cell viability (**Table 18**).

Compound	ME3 IC_{50} (µM)	Pancreatic cancer cell lines			
		BxPC-3 IC_{50} (µM)	Hs766T IC_{50} (µM)	Panc05.04 IC_{50} (µM)	Panc-1 IC_{50} (µM)
75	0.150	0.320	3.6	0.94	1.5
76	0.095	0.106	0.62	0.28	0.44

Summary

Diverse analogues with tricyclic aromatic rings were designed, synthesized and evaluated which led to compound **76** as potential dual ME3-tubulin inhibitor. Further this compound shows sub nanomolar activity on pancreatic cancer cell lines. However, these analogues have to be assessed comprehensively for their risk vs benefit ratio in *in vivo* context.

Chapter 6: Comprehensive biological evaluation protocols of selected compounds for their mechanism of action, efficacy and safety.

Details of biological evaluation studies and related protocols will be included in this chapter as following listed sections

a) *In silico*: docking studies of selected compounds with ME3 and related methodology

b) Isoform selectivity: ME2 and ME1 enzyme inhibition data for all compounds to evaluate selectivity for ME3 and related assay methodology

c) Mechanism of action: Mechanism of ME3 inhibition for compound **31** and compound **62**

d) Target engagement: Cellular thermal shift assay (CETSA) in BxPC-3 cells to demonstrate target engagement of compound **31** and compound **62** in PDAC cells with ME3.

e) In vitro off target screening: Kinome screening data for compound **31** to evaluate selectivity for ME3 to evaluate off target side effects

f) Metabolic stability: Metabolic stability study, PK studtudyy and *in vivo* BxPC-3 xenograft studies for compound **31** and related study protocol

g) Synergy study: Isobologram study of compound **62** in combination with trametinib to assess synergistic effect of this combination

Overall summary and conclusion

In summary, we have identified first in class potent and cell-active ME3 inhibitors that show selectivity over other ME isoforms. After identification and validation of compound **A** as a hit molecule, through systemic SAR studies compounds **31** and **62** were discovered and structural attributes for potent and selective inhibition of ME3 were identified. These compounds alone or in combination with other anti-cancer agents could be effective at killing PDAC cancer cells as per investigation in *in vivo* tumour xenograft model. These compounds would have therapeutic potential for the treatment of *SMAD4/ME2* deleted PDAC patients.

References

(1) Grant, T. J.; Hua, K.; Singh, A. Molecular Pathogenesis of Pancreatic Cancer. In *Progress in Molecular Biology and Translational Science*; **2016**. https://doi.org/10.1016/bs.pmbts.2016.09.008.

(2) Siegel, R. L.; Miller, K. D.; Fuchs, H. E.; Jemal, A. Cancer Statistics, 2022. *CA. Cancer J. Clin.* **2022**. https://doi.org/10.3322/caac.21708.

(3) Manji, G. A.; Olive, K. P.; Saenger, Y. M.; Oberstein, P. Current and Emerging Therapies in Metastatic Pancreatic Cancer. *Clin. Cancer Res.* **2017**. https://doi.org/10.1158/1078-0432.CCR-16-2319.

(4) Sarantis, P.; Koustas, E.; Papadimitropoulou, A.; Papavassiliou, A. G.; Karamouzis, M. V. Pancreatic Ductal Adenocarcinoma: Treatment Hurdles, Tumor Microenvironment and Immunotherapy. *World Journal of Gastrointestinal Oncology*. **2020**. https://doi.org/10.4251/wjgo.v12.i2.173.

(5) Aguirre, A. J.; Bardeesy, N.; Sinha, M.; Lopez, L.; Tuveson, D. A.; Horner, J.; Redston, M. S.; DePinho, R. A. Activated Kras and Ink4a/Arf Deficiency Cooperate to Produce Metastatic Pancreatic Ductal Adenocarcinoma. *Genes Dev.* **2003**. https://doi.org/10.1101/gad.1158703.

(6) Biswal, B. N.; Das, S. N.; Das, B. K.; Rath, R. Alteration of Cellular Metabolism in Cancer Cells and Its Therapeutic Prospects. *J. Oral Maxillofac. Pathol.* **2017**. https://doi.org/10.4103/jomfp.JOMFP_60_17.

(7) Baggetto, L. G. Deviant Energetic Metabolism of Glycolytic Cancer Cells. *Biochimie* **1992**. https://doi.org/10.1016/0300-9084(92)90016-8.

(8) Chang, Y. L.; Gao, H. W.; Chiang, C. P.; Wang, W. M.; Huang, S. M.; Ku, C. F.; Liu, G. Y.; Hung, H. C. Human Mitochondrial NAD(P)+-Dependent Malic Enzyme Participates in Cutaneous Melanoma Progression and Invasion. *J. Invest. Dermatol.* **2015**. https://doi.org/10.1038/jid.2014.385.

(9) Lu, Y. X.; Ju, H. Q.; Liu, Z. X.; Chen, D. L.; Wang, Y.; Zhao, Q.; Wu, Q. N.; Zeng, Z. lei; Qiu, H. B.; Hu, P. S.; Wang, Z. Q.; Zhang, D. S.; Wang, F.; Xu, R. H. ME1 Regulates NADPH Homeostasis to Promote Gastric Cancer Growth and Metastasis. *Cancer Res.* **2018**. https://doi.org/10.1158/0008-5472.CAN-17-3155.

(10) Liao, R.; Ren, G.; Liu, H.; Chen, X.; Cao, Q.; Wu, X.; Li, J.; Dong, C. ME1 Promotes Basal-like Breast Cancer Progression and Associates with Poor Prognosis. *Sci. Rep.* **2018**. https://doi.org/10.1038/s41598-018-35106-y.

(11) Nakashima, C.; Yamamoto, K.; Fujiwara-Tani, R.; Luo, Y.; Matsushima, S.; Fujii, K.; Ohmori, H.; Sasahira, T.; Sasaki, T.; Kitadai, Y.; Kirita, T.; Kuniyasu, H. Expression of Cytosolic Malic Enzyme (ME1) Is Associated with Disease Progression in Human Oral Squamous Cell Carcinoma. *Cancer Sci.* **2018**. https://doi.org/10.1111/cas.13594.

(12) Ren, J. G.; Seth, P.; Clish, C. B.; Lorkiewicz, P. K.; Higashi, R. M.; Lane, A. N.; Fan, T. W. M.; Sukhatme, V. P. Knockdown of Malic Enzyme 2 Suppresses Lung Tumor Growth, Induces Differentiation and Impacts PI3K/AKT Signaling. *Sci. Rep.* **2014**. https://doi.org/10.1038/srep05414.

(13) Yang, M.; Chen, X.; Zhang, J.; Xiong, E.; Wang, Q.; Fang, W.; Li, L.; Fei, F.; Gong, A. ME2 Promotes Proneural–Mesenchymal Transition and Lipogenesis in Glioblastoma. *Front. Oncol.* **2021**. https://doi.org/10.3389/fonc.2021.715593.

(14) Zhou, J. J.; Xiao, Y.; Li, H.; Wu, C. C.; Chen, D. R.; Chen, L.; Deng, W. W.; Zhang, W. F.; Sun, Z. J. Overexpression of Malic Enzyme 2 Indicates Pathological and Clinical Significance in Oral Squamous Cell Carcinoma. *Int. J. Med. Sci.* **2020**. https://doi.org/10.7150/ijms.43832.

(15) Zhang, Q.; Li, J.; Tan, X. P.; Zhao, Q. Effects of Me3 on the Proliferation, Invasion and

Metastasis of Pancreaticancer Cells through Epithelial-Mesenchymal Transition. *Neoplasma* **2019**. https://doi.org/10.4149/neo_2019_190119N59.

(16) Dey, P.; Baddour, J.; Muller, F.; Wu, C. C.; Wang, H.; Liao, W. T.; Lan, Z.; Chen, A.; Gutschner, T.; Kang, Y.; Fleming, J.; Satani, N.; Zhao, D.; Achreja, A.; Yang, L.; Lee, J.; Chang, E.; Genovese, G.; Viale, A.; Ying, H.; Draetta, G.; Maitra, A.; Wang, Y. A.; Nagrath, D.; Depinho, R. A. Genomic Deletion of Malic Enzyme 2 Confers Collateral Lethality in Pancreatic Cancer. *Nature* **2017**. https://doi.org/10.1038/nature21052.

(17) Zhang, Y. J.; Wang, Z.; Sprous, D.; Nabioullin, R. In Silico Design and Synthesis of Piperazine-1-Pyrrolidine-2,5-Dione Scaffold-Based Novel Malic Enzyme Inhibitors. *Bioorganic Med. Chem. Lett.* **2006**. https://doi.org/10.1016/j.bmcl.2005.10.065.

(18) Hsieh, J. Y.; Li, S. Y.; Tsai, W. C.; Liu, J. H.; Lin, C. L.; Liu, G. Y.; Hung, H. C. A Small-Molecule Inhibitor Suppresses the Tumor-Associated Mitochondrial NAD(P)+-Dependent Malic Enzyme (ME2) and Induces Cellular Senescence. *Oncotarget* **2015**. https://doi.org/10.18632/oncotarget.3907.

(19) Wen, Y.; Xu, L.; Chen, F. L.; Gao, J.; Li, J. Y.; Hu, L. H.; Li, J. Discovery of a Novel Inhibitor of NAD(P)+-Dependent Malic Enzyme (ME2) by High-Throughput Screening. *Acta Pharmacol. Sin.* **2014**. https://doi.org/10.1038/aps.2013.189.

(20) Ranzani, A. T.; Nowicki, C.; Wilkinson, S. R.; Cordeiro, A. T. Identification of Specific Inhibitors of Trypanosoma Cruzi Malic Enzyme Isoforms by Target-Based HTS. *SLAS Discov.* **2017**. https://doi.org/10.1177/2472555217706649.

(21) Shea, J. E. Phenotype and Genotype of Pancreatic Cancer Cell Lines. **2011**, *39* (4), 425–435. https://doi.org/10.1097/MPA.0b013e3181c15963.Phenotype.

(22) Grbovic-Huezo, O.; Pitter, K. L.; Lecomte, N.; Saglimbeni, J.; Askan, G.; Holm, M.; Melchor, J. P.; Chandwani, R.; Joshi, S.; Haglund, C.; Iacobuzio-Donahue, C. A.; Chiosis, G.; Tammela, T.; Leach, S. D. Unbiased in Vivo Preclinical Evaluation of Anticancer Drugs Identifies Effective Therapy for the Treatment of Pancreatic Adenocarcinoma. *Proc. Natl. Acad. Sci. U. S. A.* **2020**. https://doi.org/10.1073/pnas.1920240117.

(23) Shuai, W.; Wang, G.; Zhang, Y.; Bu, F.; Zhang, S.; Miller, D. D.; Li, W.; Ouyang, L.; Wang, Y. Recent Progress on Tubulin Inhibitors with Dual Targeting Capabilities for Cancer Therapy. *Journal of Medicinal Chemistry*. 2021. https://doi.org/10.1021/acs.jmedchem.1c00100.

(24) Gerlach, M.; Claus, E.; Baasner, S.; Müller, G.; Polymeropoulos, E.; Schmidt, P.; Günther, E.; Engel, J. Design and Synthesis of a Focused Library of Novel Aryl- and Heteroaryl-Ketopiperazides. *Arch. Pharm. (Weinheim).* **2004**. https://doi.org/10.1002/ardp.200400623.

(25) Waltemate, J.; Ivanov, I.; Ghasemi, J. B.; Aghaee, E.; Daniliuc, C. G.; Müller, K.; Prinz, H. 10-(4-Phenylpiperazine-1-Carbonyl)Acridin-9(10H)-Ones and Related Compounds: Synthesis, Antiproliferative Activity and Inhibition of Tubulin Polymerization. *Bioorganic Med. Chem. Lett.* **2021**. https://doi.org/10.1016/j.bmcl.2020.127687.

Mr. Gaurav Sheth

Research Student

Prof. Shailesh R. Shah

Research Supervisor